

# Celastrol inhibits laser-induced choroidal neovascularization by decreasing VEGF induced proliferation and migration

Zhen Li<sup>1</sup>, Ke-Wen Zhou<sup>1,2</sup>, Fang Chen<sup>1</sup>, Fu Shang<sup>1</sup>, Ming-Xing Wu<sup>1</sup>

<sup>1</sup>State Key Laboratory of Ophthalmology, Zhongshan Ophthalmic Center, Sun Yat-sen University, Guangzhou 510060, Guangdong Province, China

<sup>2</sup>Department of Physiology, Zhongshan School of Medicine, Sun Yat-sen University, Guangzhou 510080, Guangdong Province, China

**Correspondence to:** Ming-Xing Wu. State Key Laboratory of Ophthalmology, Zhongshan Ophthalmic Center Sun Yat-sen University No.54 Xianlie Road, Guangzhou 510060, Guangdong Province, China. wumingx@mail.sysu.edu.cn

Received: 2022-01-13 Accepted: 2022-04-13

## Abstract

• **AIM:** To evaluate celastrol's effect on choroidal neovascularization (CNV).

• **METHODS:** In this study, neovascular formation *in vitro* (tube formation and aortic ring culture) and *in vivo* (laser induced neovascular in mice) was treated with celastrol to evaluate this natural compound's impact on CNV. Western blot was applied to explore the possible mechanism for it. For *in vitro* assay, triplicate for each group was repeated at least three times. For *in vivo* assay, each group contains 5 mice.

• **RESULTS:** Celastrol suppressed tube formation and aortic ring sprout neovascularization. *In vitro* assay exhibited that celastrol inhibiting vascular endothelial growth factor (VEGF)-induced proliferation and migration of human umbilical vein endothelial cells and human choroidal endothelial cells, and by blocking VEGF signaling. Furthermore, intraperitoneal administration of celastrol significantly reduced the area of laser-induced CNV in an *in vivo* mouse model. By day 14, the area of CNV had decreased by 49.15% and 80.26% in the 0.1 mg/kg celastrol-treated group ( $n=5$ ) and in the 0.5 mg/kg celastrol treated group ( $n=5$ ), respectively, compared to the vehicle-treated group ( $n=5$ ).

• **CONCLUSION:** Celastrol inhibits CNV by inhibiting VEGF-induced proliferation and migration of vascular endothelial cells, indicating that celastrol is a potent, natural therapeutic compound for the prevention of CNV.

• **KEYWORDS:** celastrol; choroidal neovascularization; proliferation; vascular endothelial growth factor; human choroidal endothelial cells

**DOI:**10.18240/ijo.2022.08.01

**Citation:** Li Z, Zhou KW, Chen F, Shang F, Wu MX. Celastrol inhibits laser-induced choroidal neovascularization by decreasing VEGF induced proliferation and migration. *Int J Ophthalmol* 2022;15(8):1221-1230

## INTRODUCTION

Choroidal neovascularization (CNV) refers to the growth of abnormal new blood vessels from the choroid into the sub-retinal space accompanied by vascular leakage, retinal edema, and vision loss<sup>[1-2]</sup>. CNV is a major pathological change in ocular diseases that lead to blindness, such as age-related degeneration, pathologic myopia, angioid streaks, and trauma. Although the pathogenesis of CNV is not clearly understood, growth factors, such as vascular endothelial growth factor (VEGF) and fibroblast growth factor-induced cell proliferation and migration, play an important role in CNV development. Currently, anti-VEGF drugs are the most widely used treatment for CNV. Although these drugs are helpful in reducing the risk of visual deterioration, they only improve vision in 33% of patients<sup>[3-4]</sup>. Some patients experience worsening vision function, regardless of aggressive treatment with anti-VEGF agents<sup>[5-6]</sup>, suggesting other vascular mediators contribute to ocular angiogenesis. Furthermore, patients often exhibit CNV recurrence and require repeated treatments. A regimen of multiple intravitreal injections for months or years is associated with many complications, such as cataracts, retinal detachment, and endophthalmitis, as well as significant costs<sup>[7-8]</sup>. Studies have shown that participants in monthly dosing groups had a higher incidence of macular atrophy than those in discontinuous treatment groups, suggesting that anti-VEGF therapy induces the formation of macular atrophy in some patients<sup>[9-11]</sup>. To improve the outcomes of CNV treatment and reduce the cost to the patient, an alternative anti-angiogenic treatment is needed.

Celastrol, a natural products extracted from traditional Chinese herb, exhibits potent anti-inflammatory, anti-oxidant, and anti-angiogenic activities<sup>[12-15]</sup>. This drug has been widely used to treat chronic inflammation, autoimmune diseases, and many types of cancer by modulating multiple pro-angiogenic and pro-inflammatory cytokines, such as hypoxia-inducible factor-1 $\alpha$ , TNF- $\alpha$ , and VEGF<sup>[16-18]</sup>. These cytokines play a major role in the proliferation of endothelial cells and the progression of angiogenesis. Previous studies have reported that celastrol has anti-angiogenic effects on *in vitro* and *in vivo* assays<sup>[19-20]</sup>. However, few studies have evaluated the effect of celastrol on CNV. Thus, the present study investigated the effect of celastrol using a popular mouse model of laser-induced CNV.

## **MATERIALS AND METHODS**

**Ethical Approval** All animal experiments were conducted in accordance with the Statement for the Use of Animals in Ophthalmic and Vision Research and approved by the Institutional Animal Care and Use Committee of Zhongshan Ophthalmic Center. Eye cup of human beings was collected from the Eye Bank of Guangdong Province with the approval of the Sun Yat-sen University Medical Ethics Committee after getting the consent from the donor in accordance with the Declaration of Helsinki.

**Animals and the Induction of Choroidal Neovascularization** This study used 6-8 weeks old C57BL/6J mice. CNV was induced in mice by laser photocoagulation. Briefly, the procedure was performed on anesthetized [10% ketamin (100 mg/kg) and 1% xylazine (10 mg/kg) intraperitoneally] animals with dilated pupils using a laser photocoagulator (Micron IV, Phoenix Research Laboratories, Pleasanton, CA, USA) and the following parameters: spot size, 50  $\mu$ m; duration, 100ms; and power, 450 mW. Four spots were applied to each eye between the major retina vessels and around the optic disc at a distance of 1-1.5 optic disc diameters from the optic disc head. Burns that generated bubbles were included in the evaluation. Power analysis determined that 5 mice per group would provide 80% or more power to detect statistically significant differences in outcomes.

**Celastrol Treatment** Celastrol (34157-83-0, purity  $\geq$ 98%) was purchased from Desite Biology, Chengdu, China and dissolved in phosphate-buffered saline (PBS) containing 1% dimethyl sulfoxide and 10% ethanol. After laser photocoagulation, the mice were randomly divided into three groups (15 mice/group) and treated by intraperitoneal injection at a daily dose of 0.1 mg or 0.5 mg celastrol per kilogram (kg) body weight or with PBS containing 1% dimethyl sulfoxide and 10% ethanol as the vehicle control. Random numbers were generated using a computer based random order generator.

**Fluorescein Angiography and the Evaluation of Laser Induced Choroidal Neovascularization** Fluorescein

angiography (FFA) examinations were conducted on the mice to examine the laser-induced CNV. The animals were anesthetized, and their pupils were dilated as described for the induction of CNV. They were then positioned on the stage of the microscope, and hypromellose coupling fluid was applied to the eye. The camera and eye position were adjusted to ensure correct alignment and to focus on the optic nerve head plane. Standard color fundus photography was used before adjusting to the appropriate filter set for FFA; 0.1 mL/kg of 5% fluorescein sodium was then administered *via* intraperitoneal injection. Images were captured using the Micron IV (Phoenix Research Laboratories, Pleasanton, CA, USA). Images were taken at 3, 7, and 14d after laser treatment. FFA images with fluorescein administration by intraperitoneal injection were taken five minutes after fluorescein sodium was injected. Mice were sacrificed by intravenous injection of air after anesthesia 3, 7, or 14d after laser photocoagulation, and the eyecups were removed and incubated with 4% paraformaldehyde at 4°C overnight. The choroid/retinal pigment epithelium (RPE)/sclera was set in 24-well culture plates, and 0.5% bovine serum albumin (BSA) with 0.1% triton was added for 2h<sup>[21]</sup> at room temperature for blocking. After being washed with PBS, fluorescein-isothiocyanate-conjugated isolectin B4 (Vector, Burlingame, CA, USA, 1:500) was added and the sample were incubated at 4°C overnight. The fluorescence-labeling tissue was flat mounted on glass slides (ThermoFisher Scientific) and covered with a cover slip. CNV was visualized using a fluorescerin microscope (FV1000; Olympus, Tokyo, Japan). For each group at least five mice were used for result analysis.

**Cell Culture and Western Blot** Primary human choroidal endothelial cells (hCEC) were retrieved from donors with methods described before<sup>[22]</sup>. Briefly, an eye was collected from the Eye Bank of Guangdong Province within 6h from death and soaked in 0.25% povidone iodine at room temperature for 30min. After the anterior segment was removed, the choroid was isolated from the sclera with forceps, and 0.2% pronase was used for the detachment of endothelial cells. After digestion at 37°C for 4-6h, cells were collected by centrifugation. The cell pellet was resuspended in endothelial cell medium (ECM; ScienCell, USA) without serum, and CD31 beads were used to separate hCEC from the other cells. Primary cultures of human umbilical vein endothelial cells (HUVEC) were obtained and cultured as previously described<sup>[23]</sup>. The hCEC and HUVEC were cultured in completed ECM. All cells were cultured at 37°C in a humidified 5% CO<sub>2</sub> atmosphere. After treatment with VEGF or different concentrations of celastrol, the whole proteins of the hCEC and HUVEC were collected. Western blotting was performed by probing with anti-tyrosine-protein kinase (Src, 36D10, Cell Signaling Technology, USA), anti-phosphorate-

Src (D49G4, Cell Signaling Technology, USA), anti-focal adhesion kinase (FAK; D507U, Cell Signaling Technology, USA), anti-phosphor-FAK (D20B1, Cell Signaling Technology, USA), anti-protein kinase B (PKB/Akt; 11E7, Cell Signaling Technology, USA), and anti-phosphor-Akt (D9E, Cell Signaling Technology, USA). Primary antibodies were detected using goat anti-rabbit IgG conjugated with horseradish peroxidase and visualized using chemiluminescence detection reagents. At least three times batch of protein was collected and run for the western blot analysis. For cell related *in vitro* assay, five repeat was applied for each group each time and it was repeat for three times.

**Tube Formation Assay** Twenty-four well plates were precoated with 200  $\mu$ L matrigel. HUVEC and hCEC (50 000 cells/well) were seeded into each well. The cells were treated with the vehicle (1% dimethyl sulfoxide and 10% ethanol), VEGF (20 ng/mL) or different concentrations of celastrol with VEGF. Each experiment was performed in triplicate. Images of tube formation were photographed six hours post-assay under a light microscope. The data were imported as TIFF files into Image J software to calculate the total length of all tubing within each field using an angiogenesis analysis module.

**Wound Healing Assay** The monolayers of HUVEC and hCEC in 24-well cell plates were wounded by scratching with a pipette tip; they were then washed with PBS. ECM with 1% serum containing the vehicle, VEGF (20 ng/mL), or different concentrations of celastrol were added to the scratched monolayers. Images were taken under a microscope at 0, 6, 12, 24, and 36h post-wounding. Quantification was done by measuring the number of pixels in the wound area using Image J software.

**Endothelial Proliferation Assays** The HUVEC and hCEC were cultured at a density of 5000 cells/well for VEGF-induced proliferation or 10 000 cells/well for toxicity testing in 96-well plates. Cell counting kit-8 (CCK-8; Dojindo, Shanghai, China) assays were performed following the manufacturer's instructions. The OD ratio was read using BioTek's Gen5™ microplate reader (Biotek, Winooski, VT, USA) 24h after seeding.

**Aorta Ring Culture Assays** We performed an *ex vivo* angiogenesis assay similar to that described before<sup>[24]</sup>. The aorta rings from the 6-8 weeks old C57BL/6J mice were separated and cultured in ECM containing 20 ng/mL VEGF (Genzyme/Techne, Cambridge, MA) in the presence or absence of celastrol for 7d, and the sprouting of the endothelial cells was analyzed. At each time, five repeat was applied for each group and it was repeat for three times.

**Statistical Analysis and Quantification** Data are expressed as mean $\pm$ standard error of mean (SEM). All images were analyzed using Image J software (NIH). One-way analysis of

variance (ANOVA; for comparisons of three or more groups) followed by Tukey's post hoc tests were used for statistical analyses with SPSS software version 17.0 (IBM SPSS software). Statistical significance was identified as  $P < 0.05$ .

## RESULTS

**Reducing Vascular Endothelial Growth Factor-induced Neovascularization *in Vitro*** To evaluate whether celastrol prevented VEGF-induced neovascularization, two *in vitro* models of neovascularization—a tube-formation assay and an aorta-ring culture assay—were performed. As 2  $\mu$ mol/L celastrol is toxic to HUVEC<sup>[25]</sup> and both low (0.1  $\mu$ mol/L)<sup>[26]</sup> and high (1  $\mu$ mol/L)<sup>[25]</sup> inhibited migration of HUVEC, three concentration of celastrol, 0.1, 0.5, and 1  $\mu$ mol/L, were applied for this study. As shown in Figure 1, 20 ng/mL VEGF stimulated the tube formation of HUVEC and hCEC, while 0.1 and 0.5  $\mu$ mol/L celastrol significantly decreased VEGF-induced tube formation. A higher concentration of celastrol (1  $\mu$ mol/L) significantly diminished VEGF-induced HUVEC tube formation, but it had less effect on hCEC.

The aortic ring assay is a more physiologically relevant *in vitro* model for angiogenesis, as it develops blood vessels from aortic explants using the surrounding endothelial cells, which is akin to angiogenesis *in vivo*. This study found that 20 ng/mL VEGF increased both the number and length of vascular sprouting by 60%. Similar to the tube formation assay, 0.1  $\mu$ mol/L celastrol attenuated VEGF-induced vascular sprouting to the level of the control group. Although 0.5  $\mu$ mol/L celastrol decreased vascular sprouting by 30%, a statistical analysis showed no difference (Figure 2). Since 0.5  $\mu$ mol/L celastrol did not significantly decrease vascular sprouting, a higher concentration of celastrol (1  $\mu$ mol/L) was not applied to the aortic ring assay.

## Inhibitory Effect of Celastrol in Vascular Endothelial Growth Factor-Induced Endothelial Cell Proliferation and Migration

The impact of celastrol on the viability and proliferation of hCEC and HUVEC was evaluated using CCK-8 assays. No significant difference was observed between the control and celastrol-treatment groups after 24h incubation, indicating that celastrol does not have a toxic effect at these doses (Figure 3A and 3B). Although dye formation in HUVEC treated with 0.1  $\mu$ mol/L celastrol was less than in the control group, a statistical analysis found no difference among the groups. The result indicating that celastrol have no influence on viability of hCEC and HUVEC. The proliferation rates of HUVEC and hCEC were significantly enhanced by 20 ng/mL VEGF, while 0.1 and 0.5  $\mu$ mol/L celastrol obstructed the growth of cells induced by VEGF (Figure 3C and 3D). Consistent with tube formation, 1  $\mu$ mol/L celastrol attenuated VEGF-induced cell proliferation in HUVEC but not hCEC. Among the three doses of celastrol, 0.1  $\mu$ mol/L

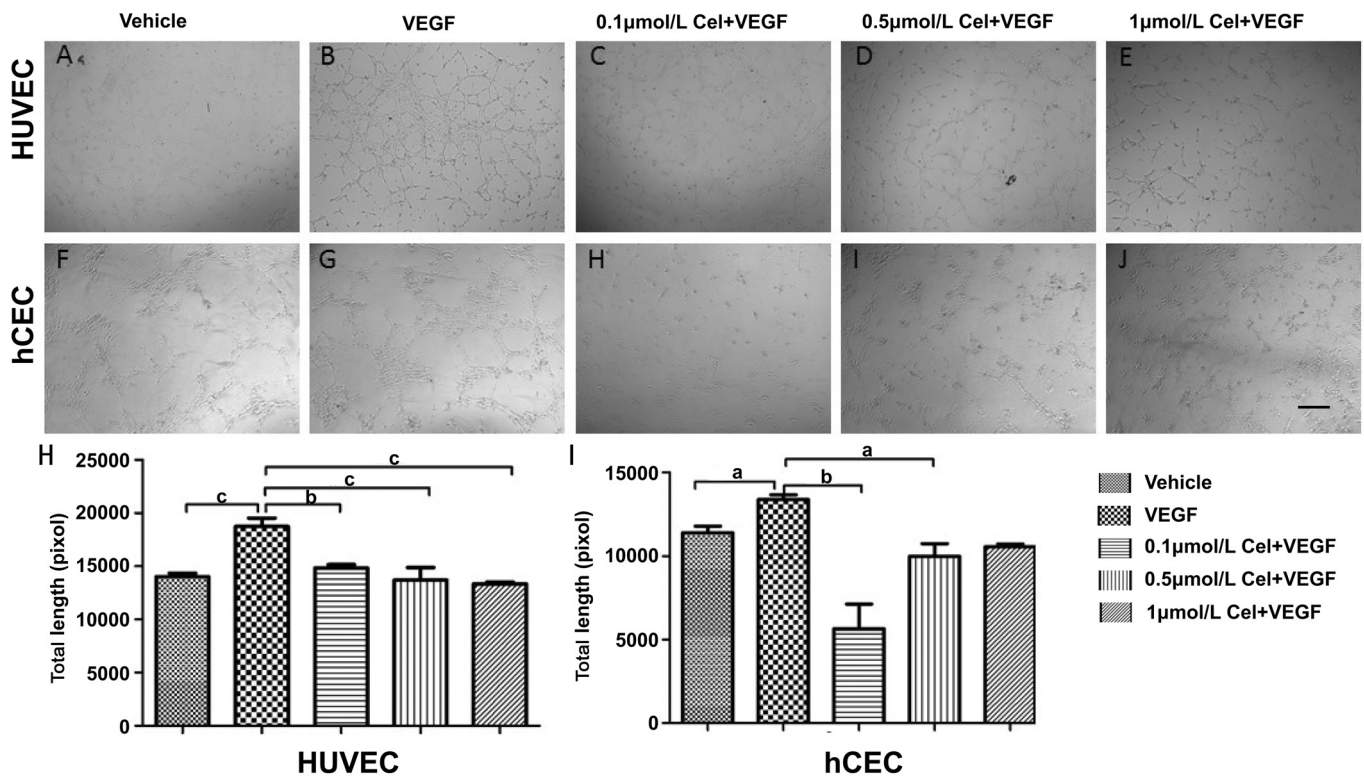


**Figure 1 Decreased tube formation of endothelial cells after treatment with celastrol** Tube formation assay was performed using primary human choroidal endothelial cells (hCEC) and primary human umbilical vein endothelial cells (HUVEC) with a vehicle, VEGF (20 ng/mL), or different concentrations of celastrol with VEGF. After 6h of incubation, images of tube formation were taken using a light microscope (A-J). The data were imported as TIFF files into Image J software to calculate the total length of all tubing within each field using an angiogenesis analysis module (H-I). Data are presented as the mean±SEM (<sup>a</sup>*P*<0.05, <sup>b</sup>*P*<0.01, <sup>c</sup>*P*<0.001, *n*=5), scale bar=200 μm.

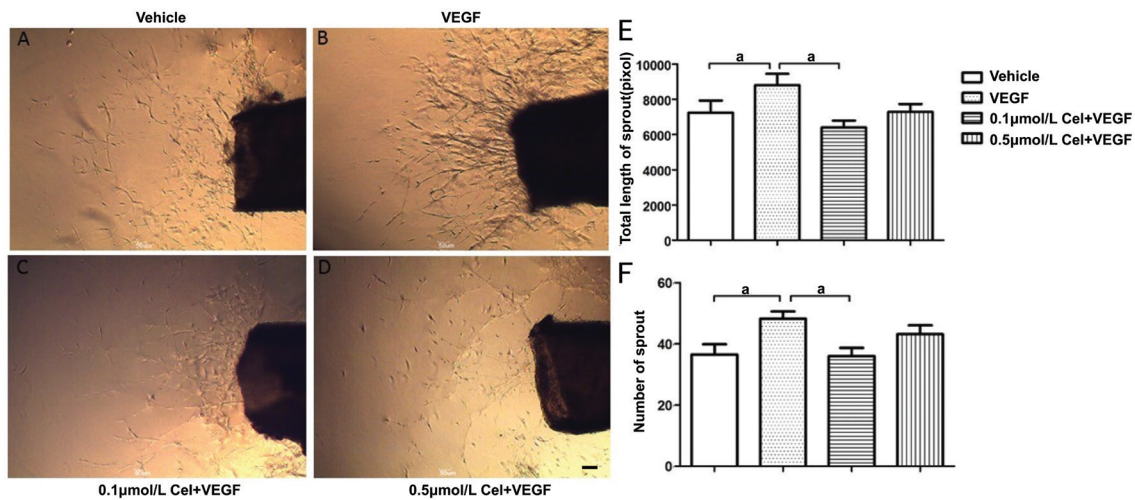


**Figure 2 Number and length of the sprout from the aortic ring attenuated by 0.1 μmol/L celastrol** The aorta rings from the 6-8 weeks old C57BL/6J mice were separated and cultured in ECM containing the vehicle (A), 20 ng/mL VEGF (B), 0.1 μmol/L celastrol with 20 ng/mL VEGF (C), and 0.51 μmol/L celastrol with 20 ng/mL VEGF (D). The phase image of the aortic ring formation was taken under a light microscope after 7d of incubation. Quantification of the aortic ring was analyzed using Image J (E-F). Data are presented as the mean±SEM (<sup>a</sup>*P*<0.05, *n*=5), scale bars=50 μm. ECM: Endothelial cell medium; VEGF: Vascular endothelial growth factor.

celastrol was shown to have the greatest ability to inhibit the function of VEGF.

**Endothelial Cell Migration in Angiogenesis** To evaluate the effect of celastrol on migration, a wound healing assay was performed. No significant difference in cell invasion

between the control and treatment groups was found during the first 12h. VEGF was shown to have a promoting effect on HUVEC and hCEC at 24h, which is similar to results reported by others<sup>[27]</sup>. At 24 and 36h, the cell-covered area in the 0.1 μmol/L celastrol group was less than in the VEGF group,

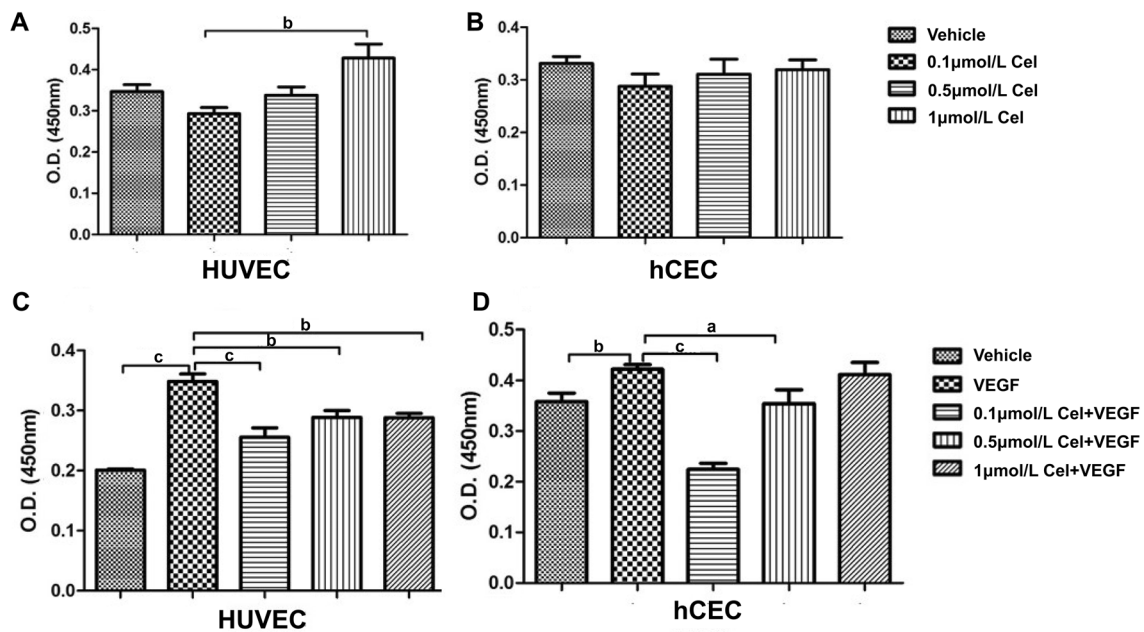


**Figure 3 Inhibition of VEGF-induced endothelial cell proliferation** HUVEC and hCEC were cultured with ECM medium containing different concentrations of celastrol for 24h, and a CCK-8 assay was performed to evaluate the potential toxicity of celastrol (A, B). The same procedure was repeated with cells treated with 20 ng/mL VEGF and celastrol diluted in a medium (C, D) to assess the effect of celastrol on VEGF-induced cell proliferation. Data are presented as the mean±SEM (<sup>a</sup> $P<0.05$ , <sup>b</sup> $P<0.01$ , <sup>c</sup> $P<0.001$ ,  $n=5$ ). HUVEC: Human umbilical vein endothelial cell; hCEC: Human choroidal endothelial cell; ECM: Endothelial cell medium; VEGF: Vascular endothelial growth factor.

indicating that 0.1  $\mu\text{mol/L}$  celastrol weakened the VEGF-induced migration of HUVEC ( $P<0.05$ ; Figure 4A and 4B). At higher concentrations of celastrol (0.5 and 1  $\mu\text{mol/L}$ ), no inhibitory effects were seen. Even 1  $\mu\text{mol/L}$  celastrol accelerate HUVEC migration at 24h. The increase in hCEC migration with VEGF treatment translated into a significant reduction at 36h with celastrol treatment (Figure 3C and 3D). Both 0.1 and 0.5  $\mu\text{mol/L}$  of celastrol restrained hCEC migration at 36h ( $P<0.001$ ). As with HUVEC, the hCEC-covered area in the 1  $\mu\text{mol/L}$  celastrol group was comparable to that of the VEGF group.

**Blocking Vascular Endothelial Growth Factor Signaling in Choroidal Neovascularization** VEGF plays a key role in the formation and growth of vascular in both physiological and pathological conditions that involve complex signaling. Expression of three major downstream proteins of VEGF signaling—FAK, Src, and Akt—and their phosphorylation were quantified by Western blotting to explore the mechanism of celastrol's inhibitory effect on neovascular formation. Western blotting demonstrated that VEGF has less effect on the expression and phosphorylation of Src and Akt in HUVEC (Figure 5A and 5B). However, an increasing trend was observed in FAK phosphorylation, while the expression of FAK was maintained in the VEGF-treated group in a time-dependent manner. In contrast, 0.5  $\mu\text{mol/L}$  celastrol diminished the FAK phosphorylation induced by VEGF after 1h of incubation. For hCEC, VEGF increased Src expression and 0.5  $\mu\text{mol/L}$  celastrol decreased it (Figure 5C and 5D).

### Inhibited CNV Leakage and Development by Celastrol

The laser-induced CNV mouse model is commonly used to evaluate the effects of treatments for CNV. To analyze the effects of celastrol *in vivo*, we calculated the area of CNV and its leakage 3, 7, and 14d after induction in mice treated with the vehicle, 0.1 mg/kg celastrol, and 0.5 mg/kg celastrol. CNV area was reduced significantly in the celastrol treatment groups ( $P<0.001$ ; Figure 6). To our surprise, as the dosage increased, so did the inhibition of celastrol on CNV ( $P<0.001$ ), which is opposite to the results of the *in vitro* experiments. On day 14, celastrol attenuated the area of CNV by 49.15% in the 0.1 mg/kg celastrol-treated group and 80.26% in the 0.5 mg/kg celastrol treated group as compared to the vehicle-treated group. In the 0.5 mg/kg celastrol group, CNV was barely seen two weeks after photocoagulation. Celastrol also decreased the leakage of CNV in a dosage-dependent manner (Figure 7). By the end of our observation, the leakage area decreased to 59.99% in the 0.1 mg/kg celastrol-treated group and 41.77% in the 0.5 mg/kg celastrol-treated group compared to the vehicle-treated group.

### DISCUSSION

In this study, we demonstrated that celastrol inhibited neovascular formation by blocking VEGF signaling and reducing VEGF-induced proliferation, migration, and tube formation of vascular endothelial cells. Our results also indicate that celastrol is a potent, natural anti-angiogenic compound for suppressing CNV development in mice. On day 3, 7, and 14 after inducing CNV, intraperitoneal administration

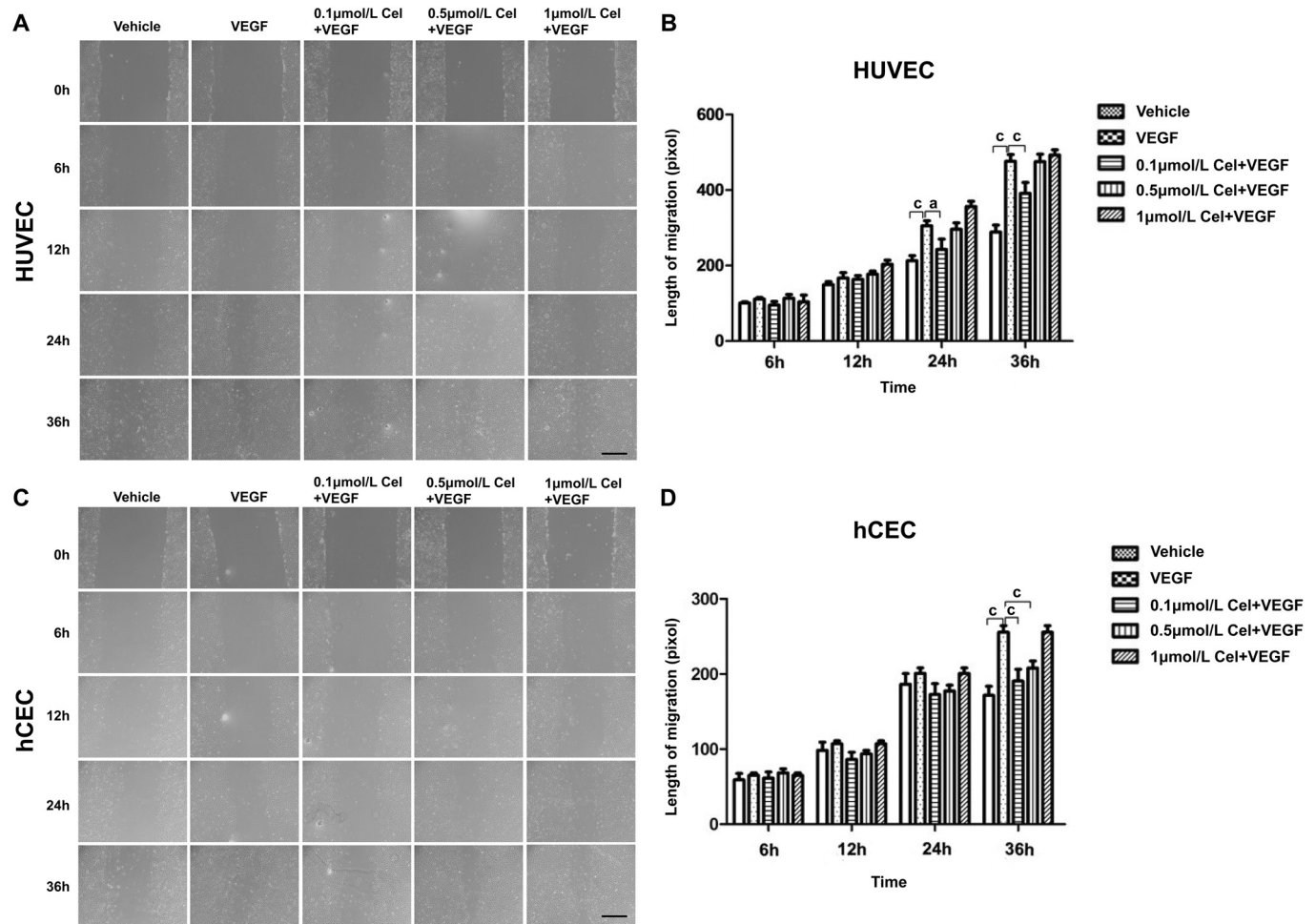


**Figure 4** The migration of endothelial cells attenuated by celastrol The monolayers of HUVEC and hCEC in 24-well cell plates were wounded by scratching with a pipette tip. ECM with 1% serum and a vehicle, VEGF (20 ng/mL), or different concentrations of celastrol were added to the scratched monolayers. Images were taken at 0, 6, 12, 24, and 36h post-wounding under a microscope for further analysis (A, C). Data are presented as the mean±SEM (<sup>a</sup>*P*<0.05, <sup>c</sup>*P*<0.001, *n*=5; B, D), scale bars=200 μm. HUVEC: Human umbilical vein endothelial cell; hCEC: Human choroidal endothelial cell; ECM: Endothelial cell medium; VEGF: Vascular endothelial growth factor.

of celastrol significantly reduced the vascular budding area and CNV leakage as seen on flat mounts of the RPE-choroid complex.

Although it is now accepted that VEGF plays a vital role in initiating and sustaining pathologic angiogenesis in the eye, animal and human studies have demonstrated that the factors involved in inflammation also contribute to these processes<sup>[28-29]</sup>. For example, the role of M2 macrophages has been reported as dominant, and they may also play an important part in the development of CNV<sup>[30]</sup>, as treatment targeting M2 polarization has been found to be effective<sup>[31-32]</sup>. Multiple clinical trials have proven that celastrol is an effective and well-tolerated drug in the treatment of inflammatory diseases<sup>[33]</sup>. Moreover, a recent *in vivo* study reported on the potent anti-angiogenic effect of celastrol in the inhibition of corneal neovascularization in rats<sup>[34]</sup>. Given its promising results as an anti-angiogenic and anti-inflammation drug, celastrol may have efficacy in treating CNV. Our results support this conclusion, as celastrol diminished neovascularization in two *in vitro* models: a tube

formation assay and an aortic ring formation assay. Moreover, mean CNV area was reduced by 49.15% in 0.1 mg/kg celastrol-treated eyes and 80.26% in 0.5 mg/kg celastrol-treated eyes compared to vehicle-treated eyes, which are similar results to those of previous studies involving other drugs, such as bevacizumab, an FDA-approved anti-VEGF drug that was reported to reduce CNV area by 80% compared to vehicle treatment in laser-induced CNV in mice<sup>[35]</sup>.

VEGF pathway activation triggers a series of signaling processes, stimulating vascular endothelial cell proliferation, survival, migration, and permeability, leading to angiogenesis and vascular leakage in pathological conditions. In the present study, two endothelial cells, HUVEC and hCEC, were exposed to 20 ng/mL VEGF or to different concentrations of celastrol. Consistent with previous report, VEGF promoted endothelial proliferation and migration<sup>[36-37]</sup>, while celastrol had a minimal effect on endothelial survival and an obvious effect on the proliferation and migration induced by VEGF; this indicates that celastrol may also play a role an anti-

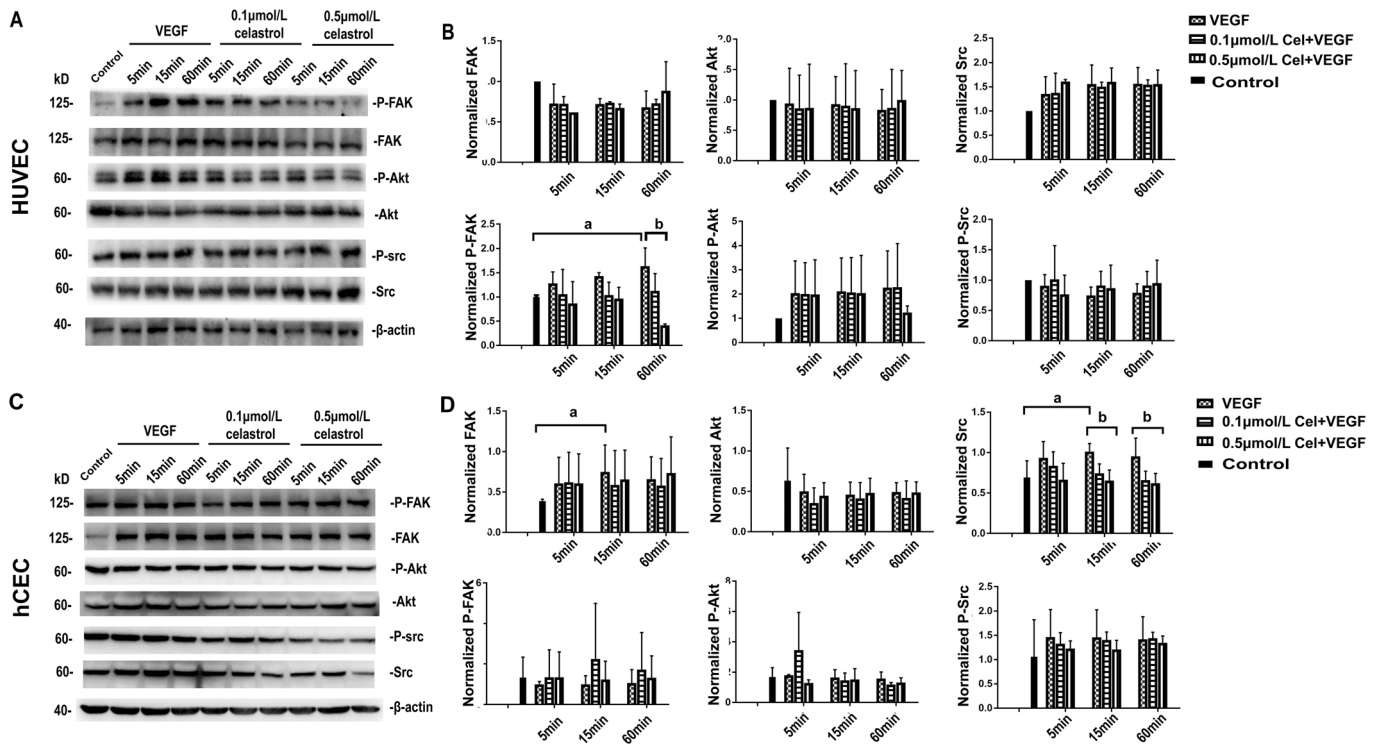


**Figure 5 Expression or phosphorylation of VEGF downstream proteins decreased by celastrol** Cell lysates from HUVEC and hCEC cultured with medium containing VEGF or celastrol were immunoblotted with anti-FAK, phosphorated FAK, Akt, phosphorated Akt, Src, or phosphorated Src antibody (A, C). FAK, Akt, and Src expression were measured using Image J and normalized with  $\beta$ -actin. Phosphorated FAK, Akt, and Src expression were measured using Image J and normalized with FAK, Akt, and Src separately (B, D). The data are presented as the mean $\pm$ SEM (<sup>a</sup> $P$ <0.05, <sup>b</sup> $P$ <0.01, <sup>c</sup> $P$ <0.001;  $n$ =3). For the image of the whole lens, the scale bar=200  $\mu$ m. For the image of the partial lens, the scale bar=50  $\mu$ m. HUVEC: Human umbilical vein endothelial cell; hCEC: Human choroidal endothelial cell; FAK: Focal adhesion kinase.

VEGF role and inhibit neovascularization by suppressing the VEGF-induced functional activity of endothelial cells. In fact, celastrol decreases VEGF expression in HUVEC under hypoxia<sup>[38]</sup> and the phosphorylation of VEGF receptor 2, which is the main signaling receptor whose activation promotes vascular endothelial cell mitogenesis and permeability<sup>[39]</sup>. Although VEGF function was restrained by celastrol in both HUVEC and hCEC, different signaling pathway activation was observed in the current study. In HUVEC, celastrol prevented FAK phosphorylation, while Src expression was decreased in hCEC, indicating that one type of endothelial cell might not represent the complexity of neovascularization *in vivo*. Both FAK and Src have been reported to mediate endothelial migration and proliferation<sup>[40-41]</sup>, while Akt has been found to be more related to cell survival<sup>[21,42-43]</sup>. This partially explains why Akt expression did not change much in either type of endothelial cell used in our study, as celastrol has a minimal effect on cell survival.

Although data from this work demonstrated celastrol's inhibitory effects in neovascularization, some results were contradictory, as celastrol *in vivo* was found to inhibit laser-induced CNV in a dose-dependent manner, while the *in vitro* experiments showed that a higher dose of celastrol (0.5

or 1 mmol/L) reduced the efficacy of celastrol to suppress VEGF-induced endothelial proliferation, migration, and tube formation, which is consistent with previous reports that lower concentrations of celastrol have a more obvious effect on VEGF suppression and the inducing activity of endothelial cells in angiogenesis<sup>[39]</sup>. One explanation for this is that the concentration of celastrol *in vivo* experiments may be lower than it *in vitro* experiments. Although we calculated the concentration of celastrol and demonstrated that 0.5 mg/kg celastrol is equal to 1 mmol/L celastrol when we treat mice as water, since the water content of mice is 73.2% of their fat-free body weight<sup>[44]</sup>. The concentration of celastrol in mice eyes may not reach 1 mmol/L because of the blood-retina barrier, which could impact drug distribution. The pharmacokinetic and pharmacodynamic properties of celastrol should be considered in future studies to assure effective dosage of celastrol for anti-neovascularization. Another possibility for the contradictory results is that our *in vitro* experiment only mimicked part of neovascularization, as the Western blot results show different signal pathway activations in the two types of endothelial cells. In summary, our study demonstrated that celastrol significantly inhibits the development of laser-induced CNV in mice. Celastrol may serve as an alternative and economical agent

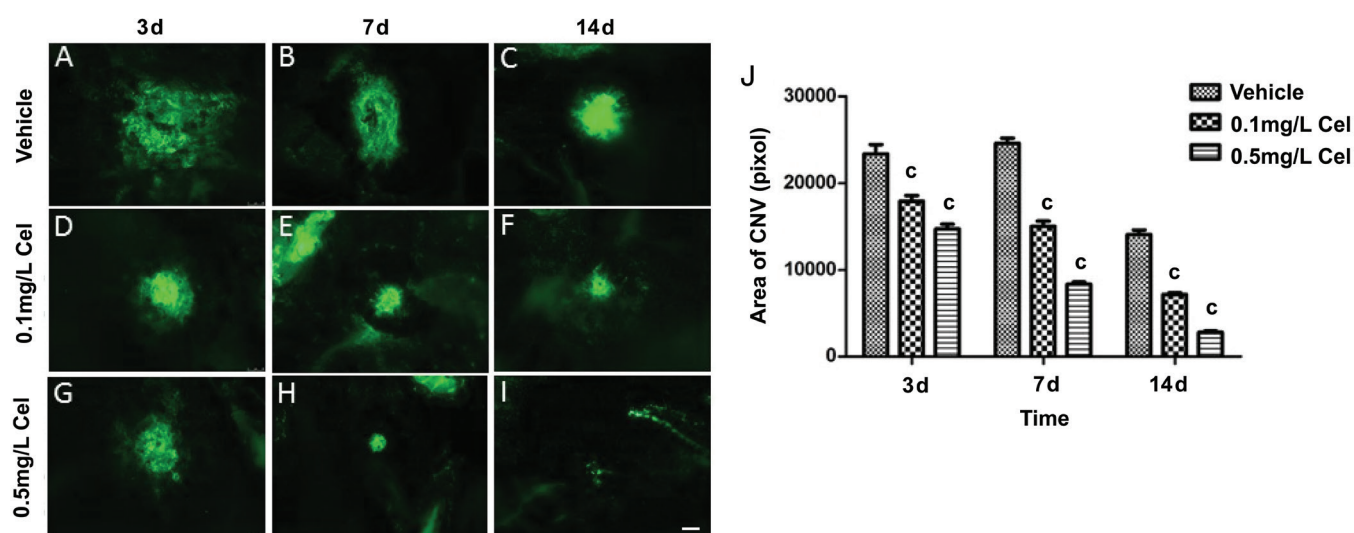


**Figure 6 Laser-induced CNV formation in mice inhibited by celastrol** The mice were treated with the vehicle, 0.1 or 0.5 mg/L celastrol after laser injury. Isolectin-B4 was used to stain RPE-choroid flat mounts of the mice 3, 7, or 14d after injury (A-I). Areas of CNV lesions were quantified using digital imaging analysis (J). Data are presented as the mean±SEM (<sup>c</sup>*P*<0.001, *n*=5). CNV: Choroidal neovascularization; RPE: Retinal pigment epithelium; SEM: Standard error of mean.

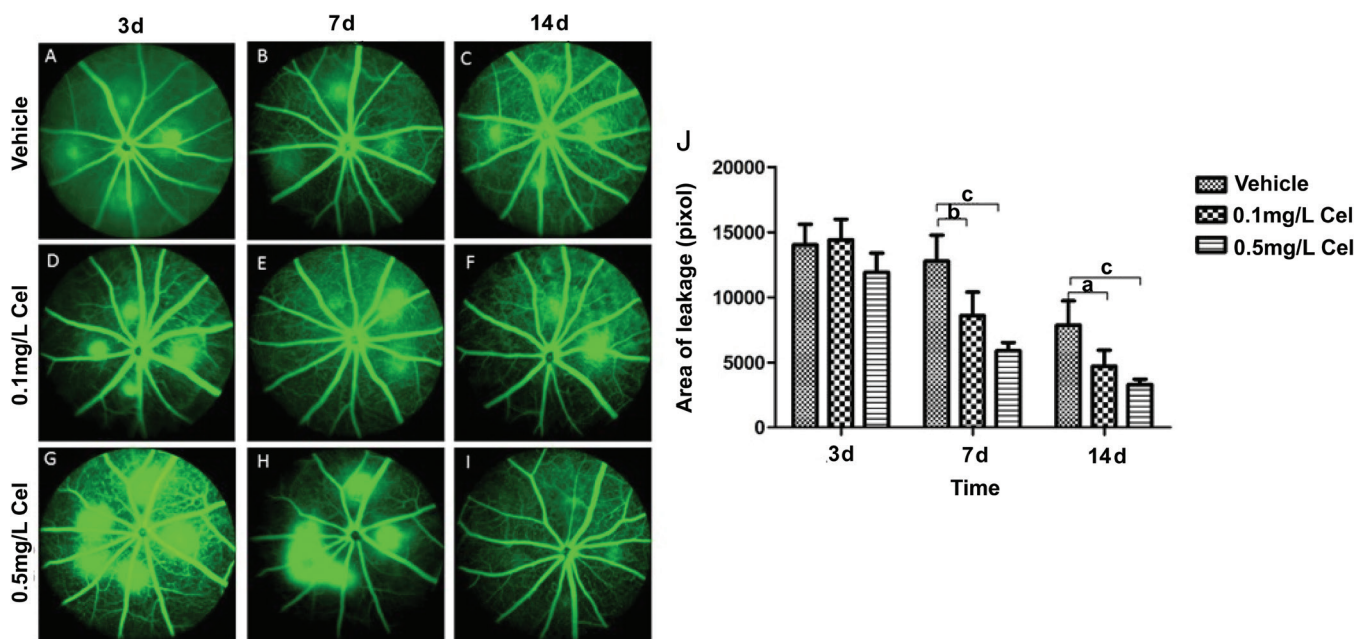


**Figure 7 The leakage of CNV decreased by celastrol** A fundus image of mice injected with 5% fluorescein sodium was taken 3, 7, and 14d after laser injury using the Micron IV system. Hyperfluorescence indicated leakage of CNV (A-I). The hyperfluorescence within lesions and avoiding choroidal vessels was measured within a defined annulus (green) around the lesion (J). Data are presented as the mean±SEM (<sup>a</sup>*P*<0.05, <sup>b</sup>*P*<0.01, <sup>c</sup>*P*<0.001, *n*=5). CNV: Choroidal neovascularization; SEM: Standard error of mean.

for CNV treatment, either alone or in conjunction with other therapies. Further studies are needed to explore the mechanism of the inhibitory effects of celastrol on angiogenesis and the optimal celastrol dose for preventing CNV.

**ACKNOWLEDGEMENTS**

The authors wish to thank Dr. Rong Ju for field assistance.

**Foundation:** Supported by National Natural Science Foundation of China (No.81570826).

**Authors' contributions:** Wu MX and Shang F prepared the manuscript. Li Z and Chen F performed analysis of the data.

Chen F was not aware of the group allocation. Li Z and Zhou KW executed the conceptualization and design of experiments. All authors read and approved the final manuscript.

**Conflicts of Interest:** Li Z, None; Zhou KW, None; Chen F, None; Shang F, None; Wu MX, None.

**REFERENCES**

1 Jensen EG, Jakobsen TS, Thiel S, Askou AL, Corydon TJ. Associations between the complement system and choroidal neovascularization in wet age-related macular degeneration. *Int J Mol Sci* 2020;21(24):9752.

- 2 Yeo NJY, Chan EJJ, Cheung C. Choroidal neovascularization: mechanisms of endothelial dysfunction. *Front Pharmacol* 2019;10:1363.
- 3 Mettu PS, Allingham MJ, Cousins SW. Incomplete response to Anti-VEGF therapy in neovascular AMD: exploring disease mechanisms and therapeutic opportunities. *Prog Retin Eye Res* 2021;82:100906.
- 4 Gil-Martínez M, Santos-Ramos P, Fernández-Rodríguez M, Abalde MJ, Rodríguez-Cid MJ, Santiago-Varela M, Fernández-Ferreiro A, Gómez-Ulla F. Pharmacological advances in the treatment of age-related macular degeneration. *Curr Med Chem* 2020;27(4):583-598.
- 5 Parodi MB, Iacono P, Da Pozzo S. Anti-VEGF and retinal dystrophies. *Curr Drug Targets* 2020;21(12):1201-1207.
- 6 Coelho J, Ferreira A, Abreu AC, Monteiro S, Furtado MJ, Gomes M, Lume M. Choroidal neovascularization secondary to pathological myopia—macular Bruch membrane defects as prognostic factor to anti-VEGF treatment. *Graefes Arch Clin Exp Ophthalmol* 2021;259(9):2679-2686.
- 7 Channa R, Sophie R, Bagheri S, Shah SM, Wang JX, Adeyemo O, Sodhi A, Wenick A, Ying HS, Campochiaro PA. Regression of choroidal neovascularization results in macular atrophy in anti-vascular endothelial growth factor-treated eyes. *Am J Ophthalmol* 2015;159(1):9-19.e2.
- 8 Solomon SD, Lindsley K, Vedula SS, Krzystalik MG, Hawkins BS. Anti-vascular endothelial growth factor for neovascular age-related macular degeneration. *Cochrane Database Syst Rev* 2019;3:CD005139.
- 9 Rieveschl NB, Song WL, Li A, Conti TF, Hom GL, Tsai GJ, Conti FF, Babiuch AS, Singh RP. Macular atrophy affecting visual outcomes in patients undergoing anti-VEGF treatment in routine clinical practice. *Ophthalmic Surg Lasers Imaging Retina* 2020;51(2):68-75.
- 10 Cho HJ, Park SM, Kim J, Nah SK, Lee J, Lee DW, Kim JW. Progression of macular atrophy in patients undergoing anti-vascular endothelial growth factor therapy for neovascular age-related macular degeneration. *Acta Ophthalmol* 2021;99(4):e540-e546.
- 11 Siedlecki J, Koch C, Schworm B, Liegl R, Kreutzer T, Kortuem KU, Schumann R, Priglinger SG, Wolf A. Enlargement rate of geographic atrophy before and after secondary CNV conversion with associated anti-VEGF treatment. *BMC Ophthalmol* 2021;21(1):1-8.
- 12 Xu SH, Feng YQ, He WS, Xu W, Xu W, Yang HJ, Li XY. Celestrol in metabolic diseases: progress and application prospects. *Pharmacol Res* 2021;167:105572.
- 13 Shi JF, Li JX, Xu ZY, Chen L, Luo RF, Zhang C, Gao F, Zhang JM, Fu CM. Celestrol: a review of useful strategies overcoming its limitation in anticancer application. *Front Pharmacol* 2020;11:558741.
- 14 Shi YN, Liu LP, Deng CF, Zhao TJ, Shi Z, Yan JY, Gong YZ, Liao DF, Qin L. Celestrol ameliorates vascular neointimal hyperplasia through Wnt5a-involved autophagy. *Int J Biol Sci* 2021;17(10):2561-2575.
- 15 Yan CY, Ouyang SH, Wang X, Wu YP, Sun WY, Duan WJ, Liang L, Luo X, Kurihara H, Li YF, He RR. Celestrol ameliorates *Propionibacterium acnes*/LPS-induced liver damage and MSU-induced gouty arthritis via inhibiting K63 deubiquitination of NLRP3. *Phytomedicine* 2021;80:153398.
- 16 Fang J, Chang XK. Celestrol inhibits the proliferation and angiogenesis of high glucose-induced human retinal endothelial cells. *Biomed Eng Online* 2021;20(1):65.
- 17 Yang F, Guo ZH, Shi LQ, Li ZR, Zhang JJ, Chai C, Li JG. Antiangiogenic and antitumor therapy for retinoblastoma with hypoxia-inducible factor-1 $\alpha$  siRNA and celestrol Co-delivery nanomicelles. *J Biomed Nanotechnol* 2020;16(10):1471-1481.
- 18 Wang H, Ahn KS, Alharbi SA, Shair OH, Arfuso F, Sethi G, Chinnathambi A, Tang FR. Celestrol alleviates gamma irradiation-induced damage by modulating diverse inflammatory mediators. *Int J Mol Sci* 2020;21(3):1084.
- 19 Nabi F, Shahzad M, Liu JY, Li K, Han ZQ, Zhang D, Iqbal MK, Li JK. Hsp90 inhibitor celestrol reinstates growth plate angiogenesis in thiram-induced tibial dyschondroplasia. *Avian Pathol* 2016;45(2):187-193.
- 20 Wang ZW, Dabrosin C, Yin X, et al. Broad targeting of angiogenesis for cancer prevention and therapy. *Semin Cancer Biol* 2015;35:S224-S243.
- 21 Abeyathna P, Su YC. The critical role of Akt in cardiovascular function. *Vasc Pharmacol* 2015;74:38-48.
- 22 Mammadzada P, Gudmundsson J, Kvanta A, André H. Differential hypoxic response of human choroidal and retinal endothelial cells proposes tissue heterogeneity of ocular angiogenesis. *Acta Ophthalmol* 2016;94(8):805-814.
- 23 Jaffe EA, Nachman RL, Becker CG, Minick CR. Culture of human endothelial cells derived from umbilical veins. Identification by morphologic and immunologic criteria. *J Clin Invest* 1973;52(11):2745-2756.
- 24 Baker M, Robinson SD, Lechertier T, Barber PR, Tavora B, D'Amico G, Jones DT, Vojnovic B, Hodivala-Dilke K. Use of the mouse aortic ring assay to study angiogenesis. *Nat Protoc* 2012;7(1):89-104.
- 25 Pang XF, Yi ZF, Zhang J, Lu BB, Sung B, Qu WJ, Aggarwal BB, Liu MY. Celestrol suppresses angiogenesis-mediated tumor growth through inhibition of AKT/mammalian target of rapamycin pathway. *Cancer Res* 2010;70(5):1951-1959.
- 26 Ni HW, Zhao WZ, Kong XT, Li HT, Ouyang J. Celestrol inhibits lipopolysaccharide-induced angiogenesis by suppressing TLR4-triggered nuclear factor-kappa B activation. *Acta Haematol* 2014;131(2):102-111.
- 27 Ke CH, Jin H, Cai JY. AFM studied the effect of celestrol on  $\beta$ 1 integrin-mediated HUVEC adhesion and migration. *Scanning* 2013;35(5):316-326.
- 28 Cunningham ET, Pichi F, Dolz-Marco R, Freund KB, Zierhut M. Inflammatory choroidal neovascularization. *Ocular Immunol Inflamm* 2020;28(1):2-6.
- 29 Do JY, Kim J, Kim MJ, Lee JY, Park SY, Yanai R, Lee IK, Park S, Park DH. Fursultiamine alleviates choroidal neovascularization by suppressing inflammation and metabolic reprogramming. *Invest Ophthalmol Vis Sci* 2020;61(12):24.
- 30 Yang Y, Liu F, Tang M, Yuan ME, Hu A, Zhan ZY, Li ZJ, Li JQ, Ding XY, Lu L. Macrophage polarization in experimental and clinical choroidal neovascularization. *Sci Rep* 2016;6:30933.

- 31 Xu Y, Cui KX, Li J, Tang XY, Lin JQ, Lu X, Huang R, Yang BY, Shi YX, Ye D, Huang JJ, Yu SS, Liang XL. Melatonin attenuates choroidal neovascularization by regulating macrophage/microglia polarization via inhibition of RhoA/ROCK signaling pathway. *J Pineal Res* 2020;69(1):e12660.
- 32 Zhao S, Lu L, Liu Q, Chen J, Yuan Q, Qiu SM, Wang X. miR-505 promotes M2 polarization in choroidal neovascularization model mice by targeting transmembrane protein 229B. *Scand J Immunol* 2019;90(6):e12832.
- 33 de Seabra Rodrigues Dias IR, Lo HH, Zhang KX, Law BYK, Nasim AA, Chung SK, Wong VKW, Liu L. Potential therapeutic compounds from traditional Chinese medicine targeting endoplasmic reticulum stress to alleviate rheumatoid arthritis. *Pharmacol Res* 2021;170:105696.
- 34 Li ZR, Li JG, Zhu L, Zhang Y, Zhang JJ, Yao L, Liang D, Wang LY. Celastrol nanomicelles attenuate cytokine secretion in macrophages and inhibit macrophage-induced corneal neovascularization in rats. *Int J Nanomedicine* 2016;11:6135-6148.
- 35 Weinberger D, Bor-Shavit E, Barliya T, Dahbash M, Kinrot O, Gatton DD, Nisgav Y, Livnat T. Mobile laser indirect ophthalmoscope: for the induction of choroidal neovascularization in a mouse model. *Curr Eye Res* 2017;42(11):1545-1551.
- 36 Apte RS, Chen DS, Ferrara N. VEGF in signaling and disease: beyond discovery and development. *Cell* 2019;176(6):1248-1264.
- 37 Zhu MH, Liu XJ, Wang Y, Chen LL, Wang L, Qin X, Xu JW, Li LL, Tu YY, Zhou TH, Sang AM, Song E. YAP *via* interacting with STAT3 regulates VEGF-induced angiogenesis in human retinal microvascular endothelial cells. *Exp Cell Res* 2018;373(1-2):155-163.
- 38 Li ZR, Guo ZH, Chu DD, Feng HY, Zhang JJ, Zhu L, Li JG. Effectively suppressed angiogenesis-mediated retinoblastoma growth using celastrol nanomicelles. *Drug Deliv* 2020;27(1):358-366.
- 39 Huang S, Tang YB, Cai XD, Peng XS, Liu XM, Zhang LJ, Xiang YC, Wang DC, Wang X, Pan T. Celastrol inhibits vasculogenesis by suppressing the VEGF-induced functional activity of bone marrow-derived endothelial progenitor cells. *Biochem Biophys Res Commun* 2012;423(3):467-472.
- 40 Zhao XF, Guan JL. Focal adhesion kinase and its signaling pathways in cell migration and angiogenesis. *Adv Drug Deliv Rev* 2011;63(8):610-615.
- 41 Ju L, Zhou ZW, Jiang B, Lou Y, Guo XR. Autocrine VEGF and IL-8 promote migration *via* src/Vav2/Rac1/PAK1 signaling in human umbilical vein endothelial cells. *Cell Physiol Biochem* 2017;41(4):1346-1359.
- 42 Wan XF, Zhu YL, Zhang LJ, Hou W. Gefitinib inhibits malignant melanoma cells through the VEGF/AKT signaling pathway. *Mol Med Rep* 2018;17(5):7351-7355.
- 43 Huang Q, Li SW, Hu XB, *et al.* Shear stress activates ATOH8 *via* autocrine VEGF promoting glycolysis dependent-survival of colorectal cancer cells in the circulation. *J Exp Clin Cancer Res* 2020;39(1):25.
- 44 Sheng HP, Huggins RA. A review of body composition studies with emphasis on total body water and fat. *Am J Clin Nutr* 1979;32(3):630-647.